

LANGEVIN SIMULATIONS IN MINKOWSKI SPACE

David J.E. CALLAWAY and Fred COOPER

Theoretical Division, Los Alamos National Laboratory 87545, USA

John R. KLAUDER

AT&T Bell Laboratories, Murray Hill, N.J. 07974, USA

Harvey A. ROSE

Theoretical Division, Los Alamos National Laboratory 87545, USA

Received 20 May 1985

A prescription is given for performing numerical simulations of field theory in Minkowski space using the Langevin equation. By introducing a weak damping term we find that the Langevin equations relax to their equilibrium values in a rather modest amount of time. As an example, we calculate the Green functions for both the harmonic and anharmonic oscillators. We study both analytically and numerically the convergence properties of $\langle x^2 \rangle$ as a function of the volume T , the time lattice spacing δ and the weak damping term ϵ . A naive Monte Carlo strategy is also considered and is shown not to converge for small ϵ .

1. Prolegomena

Approximate evaluation of euclidean space path integrals by Monte Carlo methods is commonplace at the present time [1]. However, these methods typically fail in Minkowski space calculations, where the most important part of the action is purely imaginary. Since many interesting phenomena (such as quantum tunneling) occur only in a Minkowski space formulation of field theory, it is useful to complement these standard Monte Carlo methods with techniques designed to handle an action with a significant imaginary part. Such techniques should also be useful for the study of problems such as the treatment of resonant states or of bottomless actions (which typically have no well-defined euclidean form).

Traditionally [2], in order to make sense of a Minkowski space path integral, a weak damping term is inserted by the replacement $m_0 \rightarrow m_0 - i\epsilon$, where m_0 is the bare mass of the field under consideration. The phenomena being studied then emerges in the limit of infinitesimal ϵ .

For a practical calculation, the relevant question is how small ϵ must be in order to predict this limit accurately. In a Langevin simulation the generated solution relaxes to its equilibrium value as $e^{-\epsilon\tau}$ where τ is proportional to the "time" that

the simulation runs on a computer. Thus it might be anticipated that a prohibitively large amount of computer time is required in order to examine the limit of small ϵ . However, for the cases considered here (with finite fixed volume) results obtained for ϵ of order $\frac{1}{4}$ for $m = 1$ proved sufficient to predict this limit. For a (very naïve) Monte Carlo simulation however, the importance sampling arises solely from the damping term and thus this method performs poorly in the limit of $\epsilon \sim 10$.

In what follows a preliminary examination of Langevin simulations in Minkowski space is performed. As a test problem we first consider the one-dimensional harmonic oscillator. In section 3 we also consider the anharmonic oscillator. Additionally a Monte Carlo simulation of the same problem is used as a comparison. Relative to the Langevin approach, it performs poorly.

The first problem considered is the task of estimating the path integral quotient

$$\bar{x}^2 = \frac{T^{-1} \int_0^T dt' \int \psi_0^*(x(T)) x^2(t') \exp \left(i \int_0^T \frac{1}{2}(\dot{x}^2 - x^2) dt \right) \psi_0(x(0)) Dx}{\int \psi_0^*(x(T)) \exp \left(i \int_0^T \frac{1}{2}(\dot{x}^2 - x^2) dt \right) \psi_0(x(0)) Dx}, \quad (1.1)$$

where $\psi_0(x) = \pi^{-1/4} \exp(-\frac{1}{2}x^2)$. Since ψ_0 is an eigenstate of the oscillator hamiltonian it follows that $\bar{x}^2 = \pi^{-1/2} \int x^2 \exp(-x^2) dx = \frac{1}{2}$ is the exact result. However numerical approaches to Langevin or to Monte Carlo methods cannot deal with the formal continuum path integral (1.1), and so (1.1) is replaced by its lattice-space analog given by

$$\bar{x}_L^2 = \frac{T^{-1} \sum_k \delta \int \cdots \int \psi_0^*(x_N) x_k^2 \exp \left(\frac{1}{2}i \sum \frac{(x_{l+1} - x_l)^2}{\delta} - \alpha \delta x_l^2 \right) \psi_0(x_0) Dx_N \cdots Dx_0}{\int \cdots \int \psi_0^*(x_N) \exp \left(\frac{1}{2}i \sum \frac{(x_{l+1} - x_l)^2}{\delta} - \alpha \delta x_l^2 \right) \psi_0(x_0) Dx_N \cdots Dx_0}, \quad (1.2)$$

where $\alpha \equiv 1 - i\epsilon$, $\epsilon > 0$, and ϵ represents the strength of the convergence factor (described earlier) inserted to give meaning to these integrals. For such a comparatively simple problem it is possible to compute \bar{x}_L^2 exactly for fixed δ , ϵ and N (where $T = \delta N$), and thus we are able to make a direct comparison of the Langevin equation and Monte Carlo method predictions for \bar{x}_L^2 . This is especially useful since it enables meaningful estimates of the dependence of the convergence rate δ , ϵ and N to be given. Besides an extensive analysis of the harmonic oscillator problem we have also studied several properties of a real-time (quartic) anharmonic oscillator model.

In sec. 2 the Langevin formalism is reviewed, while in sect. 3 numerical results are presented. A brief comment on comparisons with Monte Carlo methods is made in sect. 4 and conclusions are given in sect. 5.

2. Langevin equation approach

2.1. PRELIMINARIES

The Langevin equation scheme [3] is based originally on the fact that the equilibrium (stationary) distribution of the Langevin equation

$$\frac{du}{d\tau}(\tau) = -\partial A(u(\tau))/\partial u + \eta(\tau) \quad (2.1)$$

is given by $\rho(u) = N^{-1} \exp[-A(u)]$ provided that A is real and $N \equiv \int \exp(-A) du < \infty$. Here η is a gaussian white noise chosen so that $\langle \eta(\tau) \rangle = 0$ and $\langle \eta(\tau) \eta(\sigma) \rangle = 2\delta(\tau - \sigma)$. Thus the solution $u(\tau)$ provides an alternate (to Monte Carlo) importance-sampled path for which

$$T^{-1} \int_0^T F(u(\tau)) d\tau \quad (2.2)$$

provides a statistical estimate of

$$\bar{F} = \int F(u) e^{-A(u)} du / \int e^{-A(u)} du. \quad (2.3)$$

The validity of this approach arises [4] because a general solution $P(u, \tau)$ of the Fokker-Planck equation,

$$\frac{\partial P(u, \tau)}{\partial \tau} = \frac{\partial}{\partial u} \left(\frac{\partial}{\partial u} + \frac{\partial A(u)}{\partial u} \right) P(u, \tau), \quad (2.4)$$

subject to the normalized initial condition $P(u, 0) = P_0(u)$, has the asymptotic behavior

$$P(u, \tau) \underset{\tau \rightarrow \infty}{\approx} N^{-1} e^{-A(u)}. \quad (2.5)$$

Indeed for typical A 's of interest the general solution admits the representation

$$\begin{aligned} P(u, \tau) &= \sum_{n=0}^{\infty} P_n(u) e^{-E_n \tau} \\ &= N^{-1} e^{-A(u)} + \sum_{n=1}^{\infty} P_n(u) e^{-E_n \tau}, \end{aligned} \quad (2.6)$$

where

$$\frac{d}{du} \left(\frac{d}{du} + \frac{dA(u)}{du} \right) P_n(u) = E_n P_n(u). \quad (2.7)$$

Since $\rho(u) = P_0(u)$ (with $E_0 = 0$) is non-vanishing it is easy to see (e.g. from Sturm-Liouville theory) [5] that $E_n > 0$ for $n \geq 1$.

If A becomes complex, but still such that $\int |\exp(-A)| du < \infty$, then the foregoing analysis applies in many cases. In particular, the solution of (2.1) becomes complex although the noise remains real as before. The validity of (2.2) as an estimate of (2.3) still depends on the asymptotic condition (2.5), which in turn holds whenever $\text{Re}(E_n) > 0$ for $n \geq 1$. Unfortunately this constraint on the eigenvalues is not always true [5], however, there is strong evidence (from perturbation theory [7] and numerical examples) [6] that the desired conditions hold whenever A_2 , the quadratic part of A , is already stable, i.e. when $\int |\exp(-A_2)| du < \infty$. For the problems of interest to us we expect the application of the complex Langevin equation to be valid.

2.2. FORM OF THE LANGEVIN EQUATIONS

The Langevin equation appropriate to (1.2) is an $(N+1)$ -fold vector equation for the $N+1$ complex functions of the auxiliary time $z_l(\tau)$, $l = 0, \dots, N$. We use the notation $z (= x + iy)$ to emphasize that the solution is complex, unlike the real variables that appear in the integral (1.2). The Langevin equations themselves are then given, for $0 \leq l \leq N$, by

$$\begin{aligned} \frac{d}{d\tau} z_l(\tau) = & (i/\delta^2) [(2 - e_l) z_l(\tau) - z_{l+1}(\tau) - z_{l-1}(\tau)] - i\alpha z_l(\tau) \\ & - e_l z_l(\tau)/\delta + \eta_l(\tau). \end{aligned} \quad (2.8)$$

In this equation $z_{-1} \equiv z_{N+1} \equiv 0$, $e_0 = e_N \equiv 1$ with all other $e_l \equiv 0$, and η_l are a set of independent gaussian white noises for which $\langle \eta_l(\tau) \rangle = 0$ and $\langle \eta_l(\tau) \eta_m(\sigma) \rangle = 2\delta_{lm}\delta(\tau - \sigma)/\delta$. Observe that the lattice-space path integral (1.2) is not a trace but a fixed matrix element and that the latter e_l terms just incorporate the initial and final gaussian wave function. For a non-gaussian wave function, the derivative of $\ln \psi$ would appear at $n = 0, N$. For the quartic anharmonic oscillator with lagrangian given by

$$\frac{1}{2}(\dot{x}^2 - x^2) - gx^4/4!, \quad g \geq 0, \quad (2.9)$$

the preceding Langevin equations are changed by the addition of a term $-\frac{1}{6}igz^3(\tau)$ on the right-hand side. In either case these equations are to be solved for $\tau > 0$ subject to some initial condition $z_l(0)$ at $\tau = 0$. For T in (2.2) sufficiently great the estimate should be essentially independent of the initial condition.

To solve the coupled Langevin equations we have used a simple first-order Euler scheme, a second-order Runge-Kutta scheme developed by Helfand [8], and another method which exactly integrates the non-linearities. Comments on the relative merits of these algorithms appear in sect. 3.

2.3. DIRECT EVALUATION OF \bar{x}_L^2

As noted earlier, for the harmonic oscillator, the continuum value of \bar{x}^2 is $\frac{1}{2}$, but this will not be the case for \bar{x}_L^2 . However, it is straightforward to determine, at least numerically, the value of \bar{x}_L^2 for any choice of N , δ and ε . The denominator in (1.2) may be written in the form

$$I \equiv \int \cdots \int \exp \left(-\frac{1}{2} \sum A_{kl} x^k x^l \right) \prod dx_n = \text{const}/(\det A)^{1/2}, \quad (2.10)$$

where A is the $(N+1) \times (N+1)$ matrix which can be read off from (1.2). To determine \bar{x}_L^2 we note that

$$\bar{x}_L^2 = \frac{2i}{T} \frac{d}{d\alpha} \ln I = \frac{-i}{T} \text{Tr} \left(A^{-1} \frac{d}{d\alpha} A \right) = \frac{-i}{T} \frac{d(\det A)/d\alpha}{\det A}.$$

Since A is tridiagonal the determinant is readily found from a three-term recursion relation.

2.4. SOLUTION OF THE LANGEVIN EQUATION

Before entering into a discussion of a discrete version of the path integral it is useful to solve exactly the continuum equation for the one-dimensional harmonic oscillator [cf. eq. (2.1)],

$$\frac{d}{d\tau} x(\tau, \varepsilon) + \varepsilon x = -i \left(\frac{d^2}{dt^2} x + m^2 x \right) + \eta(t, \tau), \quad (2.11a)$$

where x is complex and

$$\langle \eta(t_1, \tau_1) \eta(t_2, \tau_2) \rangle = 2\delta(t_1 - t_2) \delta(\tau_1 - \tau_2). \quad (2.11b)$$

The Fourier transform of eq. (2.11a) yields

$$\langle x(k_1, \tau) x(k_2, \tau) \rangle = \frac{2\pi i \delta(k_1 + k_2)}{k_1^2 - m^2 + i\varepsilon} [1 - e^{-2\varepsilon\tau} e^{i2(k_1^2 - m^2)\tau}], \quad (2.12)$$

where

$$x(k_1, \tau) = \int e^{ik_1 t} x(t, \tau) dt. \quad (2.13)$$

Eq. (2.12) shows that in the continuum limit the relaxation time is proportional to ε^{-1} in Minkowski space and not $(k_1^2 + m^2)^{-1}$ as in Euclidean space.

At finite ε , $x(k, \tau)$ has both real and imaginary parts $x(k, \tau) = u(k, \tau) + iv(k, \tau)$ and therefore

$$\begin{aligned}
 \langle u(k, \tau)u(k', \tau) \rangle &= 2\pi\delta(k-k')[1 - e^{-2\varepsilon\tau}]/2\varepsilon \\
 &\quad + \frac{2\pi\delta(k+k')}{2[\varepsilon^2 + \alpha^2]} [\varepsilon + e^{-2\varepsilon\tau}(\alpha \sin 2\alpha\tau - \varepsilon \cos 2\alpha\tau)], \\
 \langle v(k, \tau)v(k', \tau) \rangle &= 2\pi\delta(k-k')[1 - e^{-2\varepsilon\tau}]/2\varepsilon \\
 &\quad \times \frac{-2\pi\delta(k+k')}{2[\varepsilon^2 + \alpha^2]} [\varepsilon + e^{-2\varepsilon\tau}(\alpha \cos 2\alpha\tau + \varepsilon \sin 2\alpha\tau)], \\
 \langle u(k, \tau)v(k', \tau) \rangle &= 2\pi \frac{\delta(k+k')}{2(\varepsilon^2 + \alpha^2)} [\alpha - e^{-2\varepsilon\tau}(\alpha \cos 2\alpha\tau + \varepsilon \sin 2\alpha\tau)], \\
 \alpha &= p^2 - m^2.
 \end{aligned} \tag{2.14}$$

It follows that

$$\text{Re} \langle x^2(k, \tau) \rangle = \langle u^2(k, \tau) \rangle - \langle v^2(k, \tau) \rangle \tag{2.15}$$

is the difference between two possibly large numbers since both u^2 and v^2 go as $1/\varepsilon$ for large τ .

If the t -axis is made discrete ("put on a lattice"), the result is

$$\begin{aligned}
 x(t, \tau) &= \frac{1}{T} \sum_{-N/2}^{N/2} e^{ik_n t} \tilde{x}(k_n, \tau), \\
 T &\equiv N\delta, \quad k_n = \frac{2\pi n}{T} = \frac{2\pi}{\delta} \frac{n}{N}, \quad t_m = m\delta,
 \end{aligned} \tag{2.16a}$$

$$\tilde{x}(k, \tau) = \sum_{m=-N/2}^{N/2} \exp(-it_m) x(t_m, \tau). \tag{2.16b}$$

Defining the oscillator on a lattice results in the replacements

$$\alpha = (k^2 - m^2) \rightarrow \alpha_n \equiv \frac{2}{\delta^2} [1 - \cos(k_n \delta)] - m^2, \tag{2.17a}$$

$$\delta(k+k') \rightarrow \frac{T}{2\pi} \delta_{k+k'}. \tag{2.17b}$$

It follows from the above discussion that the equilibrium propagator for the lattice harmonic oscillator is

$$\langle x(k)x(-k) \rangle = \frac{T}{\alpha_n + i\varepsilon} = T \left[\frac{\alpha_n}{\alpha_n^2 + \varepsilon^2} - \frac{i\varepsilon}{\alpha_n^2 + \varepsilon^2} \right]. \tag{2.18}$$

In order to present a method of performing calculations in Minkowski space it is first necessary to identify a suitable test problem. An appropriate candidate is the evaluation of the expectation value $\langle x^2 \rangle$.

In the continuum

$$\langle x^2 \rangle = \frac{i}{2\pi} \int \frac{dp}{p^2 - m^2 + i\epsilon}. \quad (2.19)$$

At finite ϵ this integral can be done exactly, giving

$$\text{Re} \langle x^2 \rangle = \frac{\epsilon}{2\pi} \int_{-\infty}^{\infty} \frac{dp}{(p^2 - m^2)^2 + \epsilon^2} \quad (2.20a)$$

$$= \frac{\sqrt{2}}{4\epsilon\xi} (\xi - 1)^{1/2} (\xi + 1), \quad (2.20b)$$

where

$$\xi \equiv \frac{(\epsilon^2 + m^2)^{1/2}}{m}. \quad (2.20c)$$

(In the sequel m is set to unity). Eq. (2.20b) can be expanded for small ϵ to yield

$$\text{Re} \langle x^2 \rangle = \frac{1}{2} - \frac{3}{16}\epsilon^2 + \dots \quad (2.21)$$

This expansion is quite accurate for $\epsilon \leq \frac{3}{8}$.

The imaginary part of the integral eq. (2.19) can also be calculated,

$$\text{Im} \langle x^2 \rangle = \frac{\sqrt{2}}{4\xi} (\xi - 1)^{1/2} \quad (2.22)$$

$$= \frac{1}{4}\epsilon - \frac{5}{32}\epsilon^3 + \dots \quad (2.23)$$

The lattice versions of eqs. (2.20) and (2.22) are

$$\text{Re} \langle x^2 \rangle = \frac{\epsilon}{T} \sum_{n=-N/2}^{N/2} (\alpha_n^2 + \epsilon^2)^{-1}, \quad (2.24a)$$

$$\text{Im} \langle x^2 \rangle = \frac{1}{T} \sum_{n=-N/2}^{N/2} \frac{\alpha_n}{(\alpha_n^2 + \epsilon^2)}, \quad (2.24b)$$

where α_n is as defined in eq. (2.17a). These quantities depend upon the time lattice spacing δ as well as the “volume” $T \equiv N\delta$ and the cutoff ϵ .

For small ϵ and fixed δ and T , $\text{Re} \langle x^2 \rangle_{\delta, T}$ has a maximum at finite ϵ . This is because if one does not exactly pick up the pole (2.24a) goes to zero with ϵ . The interesting questions are, “At what ϵ we approach the $\epsilon = 0$ result?”, and, “At what volume are we approaching the infinite-volume limit?” In fig. 1 we plot at a lattice spacing $\delta = \frac{1}{2}$, $\langle x^2(\epsilon) \rangle$ for volume $T = 10, 20, 40$. We see that at $T = 20$ we are already getting a few percent accuracy at the maximum which occurs around $\epsilon = 0.2$.

In fig. 2 we plot the approach to the continuum limit at finite volume, $T = 20$. We see that having the lattice spacing $\delta = \frac{1}{4}$, ($T = N\delta$) is almost indistinguishable from $\delta = \frac{1}{2}$. We also again see that quite accurate answers are obtained even at $\delta = \frac{1}{2}$

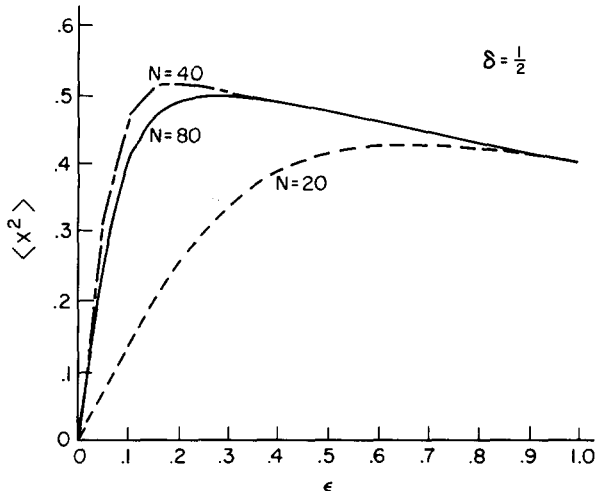


Fig. 1. $\text{Re} \langle x^2 \rangle$ versus ϵ at lattice spacing $\delta = \frac{1}{2}$, for volume $T = 10, 20, 40$; $g = 0$.

for $\epsilon = 0.3$. Thus we find that it is only necessary to achieve $\epsilon \sim \frac{1}{4}$ to obtain numerically accurate results in the free-field case. This requires only four times the simulation time as a euclidean problem, since there $\tau \sim 1/m$ and $m = 1$.

3. Numerical results for the harmonic and anharmonic oscillators

We want to solve eq. (2.8) for the free-field case or in the anharmonic oscillator case we have an extra $-\frac{1}{6}igz_i^3(\tau)$ on the right-hand side. The generic equation is of

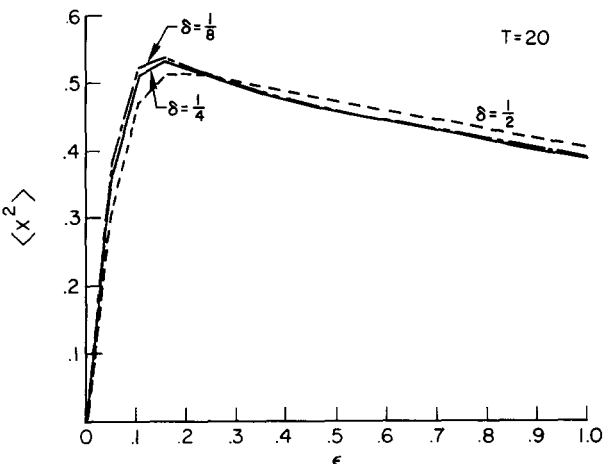


Fig. 2. $\text{Re} \langle x^2 \rangle$ versus ϵ at $T = 20$ for lattice spacings $\delta = \frac{1}{2}, \frac{1}{4}, \frac{1}{8}$; $g = 0$.

the form

$$\dot{z}_l(\tau) = F_l(z(\tau)) + \eta_l(\tau). \quad (3.1)$$

A first-order differential equation solver replaces this equation by ($\tau_n = nh$):

$$z_l(n+1) = z_l(n) + F_l(z(n))h + \bar{\eta}_l(n), \quad \bar{\eta}_l = \eta_l h. \quad (3.2a)$$

The noise

$$\bar{\eta}_l(n) = \frac{\sqrt{2h}}{\delta} y_l(n), \quad (3.2b)$$

where the $y_l(n)$ are random gaussian noise normalized to one. We use the standard algorithm for generating gaussian noise normalized to one. Suppose U_1 and U_2 are two independent random numbers (uniformly distributed) between zero and one and

$$\begin{aligned} \alpha_1 &= (-2 \log U_1)^{1/2} \cos(2\pi U_2), \\ \alpha_2 &= (-2 \log U_1)^{1/2} \sin(2\pi U_2) \end{aligned} \quad (3.3)$$

are two independent unit-variance gaussian-distributed random numbers (which we use as the $y_l(n)$). Since a first-order method is accurate to order h and thus might require many iterations we have also used a second-order method good to order h^2 so that larger time steps could be used.

The second-order Runge-Kutta [8] algorithm we used was to let

$$\begin{aligned} w_{1l} &= F_l(z(n)), \\ w_{2l} &= F_l(z(n) + hw_{1l} + \bar{\eta}_l(n)), \\ z_l(n+1) &= z_l(n) + \frac{1}{2}h(w_{1l} + w_{2l}) + \bar{\eta}_l(n), \end{aligned} \quad (3.4)$$

where again

$$\bar{\eta}_l = \frac{\sqrt{2h}}{\delta} y_l.$$

For the anharmonic oscillator, the above two methods are unstable for large g and small ε .

To avoid this problem we also used a two-step integration scheme which takes into account the non-linearities exactly.

We have

$$\dot{z}_l(\tau) = \frac{i}{\delta^2} [(2 - e_l) z_l(\tau) - z_{l+1}(\tau)] - i\alpha z_l(\tau) - e_l \frac{z_l}{\delta}(\tau) + \eta_l(\tau) - \frac{1}{6}ig z_l^3(\tau). \quad (3.5)$$

If we first integrate just the non-linear term exactly we obtain

$$z_l(\tau) = \frac{z_l(0)}{\sqrt{1 + z_l^2(0) \frac{1}{3}ig\tau}}. \quad (3.6)$$

Then we first set

$$\bar{z}_{\text{old}} = \frac{z_{\text{old}}}{\sqrt{1 + z_{\text{old}}^2 \frac{1}{3} i g h}} \quad (3.7)$$

and finally use

$$z_{\text{new}} = \bar{z}_{\text{old}} + \tilde{F}(\bar{z}_{\text{old}})h + \bar{\eta}_l, \quad (3.8)$$

or eq. (3.4) with z_{old} replaced by \bar{z}_{old} , and F by \tilde{F} where \tilde{F} contains only the linear terms. It is clear that to order h the update (3.7)–(3.8) agrees with (3.2).

After we determined $x(t, \tau)$, where $t = k\delta$, $\tau = nh$ after a certain number of iterations $n = I$, we then determine the following average quantities:

$$\bar{A}_I = \sum_{k=1}^N \sum_{n=i}^I \frac{A(k\delta, nh)}{(I-i)N}, \quad (3.9)$$

where

$$\begin{aligned} x(t, \tau) &= u(t, \tau) + iv(t, \tau), \\ A &= u, v, u^2, v^2, \quad \text{Re } x^2 = u^2 - v^2, \end{aligned}$$

and

$$\text{Im } x^2 = 2uv.$$

We throw out the first i (typically 1000) iterations. In our simulations we start from an aligned initial configuration $x(k\delta, 0) = 1$.

We also determine the Fourier transform

$$x(k, \tau) = a \sum_{n=-N/2}^{N/2} e^{-ik(n\delta)} x(n\delta, \tau) \quad (3.10)$$

and calculated after I iterations

$$\overline{x(k, \tau)x(-k, \tau)} = \sum_{n=i}^I \frac{x(k, nh)x(-k, nh)}{(I-i)}, \quad (3.11)$$

which we compared with both the real and imaginary parts of eq. (2.18). In solving the differential equation one must choose $\Delta\tau = h \leq (\Delta t)^2 = \delta^2$. It also is true in the nonlinear case that for numerical stability as ϵ gets smaller one needs to decrease h at fixed T, δ .

For the harmonic oscillator we used both the Euler method and the second-order Runge–Kutta method to solve (2.8). In general the second-order method was five times faster since it tolerated a much coarser $\Delta\tau$ to be stable and still converge to the correct answer. For example at $\epsilon = 1$, $T = 10$, $\delta = \frac{1}{4}$, one required $h = 0.0001$ for the first-order method and $h = 0.0005$ for the second-order method to be numerically accurate ($\leq 1\%$).

For the harmonic case we chose to compare the numerical simulation with the cases shown in figs. 1 and 2. That is we studied the case $T = 10$ and $\delta = \frac{1}{4}, \frac{1}{8}$ as well as $T = 20$, $\delta = \frac{1}{4}$. We found that there were different relaxation times for the measured qualities. $\langle u \rangle$ and $\langle v \rangle$ rapidly go to zero. Next $\langle u^2 \rangle$ and $\langle v^2 \rangle$ stabilize and as expected are of order $1/\varepsilon$ in magnitude. Then $\text{Re} \langle x^2 \rangle = \langle u^2 - v^2 \rangle$ stabilizes. We found that we needed $\langle u^2 \rangle$ and $\langle v^2 \rangle$ to be stable to 1% before $\text{Re} \langle x^2 \rangle$ was stable to 5%. Lastly the momentum space propagator relaxed to its equilibrium value.

Table 1 summarizes the results of the second two algorithms at various ε between 0.35 and 2. One sees that to get similar accuracy as we decrease ε we need many more iterations (increasing τ and decreasing h). If we do not decrease h with ε , the iteration scheme is not accurate.

Similar results were obtained from the first-order Euler method but the number of iterations needed was greater by a factor anywhere from 3-10.

At $g = 1$ the first-order method developed instabilities at $\varepsilon \leq 1.5$. The second-order method became unstable at $g = 1$ for $\varepsilon \leq 0.5$ at $N \geq 40$. We therefore used at small ε , the method outlined by equations (3.5)-(3.8). This third method agreed to 0.1% with the second-order Runge-Kutta and had the virtue of being stable at all ε .

In table 1 we compare a simulation at $g = 0$ with one at $g = 1$ to show that the number of iterations needed for 10% numerical stability was quite similar. One

TABLE 1
A comparison of simulations at $g = 0$ and $g = 1$, $N = 40$, $\delta = \frac{1}{4}$, $T = 10$ for
 $\langle x^2 \rangle$ as a function of ε

ε	$\langle x^2 \rangle$ exact, $g = 0$	$\langle x^2 \rangle$ simulation, $g = 0$	$\langle x^2 \rangle$ simulation, $g = 1$
$\varepsilon = 2$	0.306	$I = 15\ 000$	$I = 25\ 000$
		0.305 ± 0.005	0.28 ± 0.01
		$h = 0.001$	$h = 0.0005$
$\varepsilon = 1.5$	0.334	$I = 20\ 000$	$I = 30\ 000$
		0.332 ± 0.005	0.327 ± 0.010
		$h = 0.0005$	$h = 0.0005$
$\varepsilon = 1.0$	0.390	$I = 35\ 000$	$I = 50\ 000$
		0.385 ± 0.010	0.349 ± 0.010
		$h = 0.0003$	$h = 0.0003$
$\varepsilon = 0.5$	0.4825	$I = 100\ 000$	$I = 200\ 000$
		0.476 ± 0.020	0.459 ± 0.03
		$h = 0.0002$	$h = 0.0001$
$\varepsilon = 0.35$	0.35	$I = 120\ 000$	$I = 250\ 000$
		0.38 ± 0.03	0.43 ± 0.03
		$h = 0.00015$	$h = 0.0001$

I = number of iterations. $h = \Delta\tau$. $Ih = \tau$.

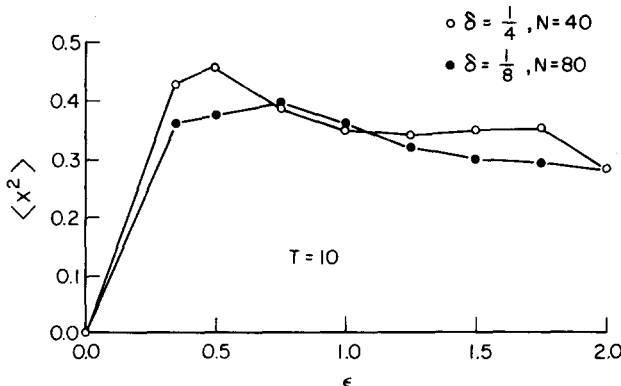


Fig. 3. Simulation for $\text{Re} \langle x^2 \rangle$ versus ϵ . $g = 1$, $T = 10$, for $\delta = \frac{1}{4}, \frac{1}{8}$ ($T = N\delta$).

needed (in general) relaxation times that were 1–2 times greater for the anharmonic case to obtain similar accuracy.

In fig. 3 we present the numerical results for $\text{Re} \langle x^2 \rangle$ versus ϵ at different volumes for the value of $g = 1$. We notice these curves are quite similar to their free-field theory counterparts. We have also run a euclidean space Langevin simulation for $\langle x^2 \rangle$ at $\epsilon = 0$, $T = 10$ and obtained $\langle x^2 \rangle = 0.43 \pm 0.03$. We see that the Minkowski space simulation at $\epsilon = 0.5$ is consistent with this result.

In order to perform these calculations we used both a VAX 780 and a Cray XMP. On the Cray a simulation at large $\epsilon \geq 1.5$ took around 20 seconds of CPU time. To get accurate results at $\epsilon = 0.35$, $g = 1$ took 20 minutes of CPU time on the Cray. No attempt was made to optimize the calculation. For calculations of the mass, using Fourier space techniques are expected to drastically shorten the computation time.

4. Naïve Monte Carlo simulation

There are, of course, numerous other algorithms for the simulation of quantum systems. Most notable amongst these are Monte Carlo methods (reviewed in ref. [9]) and microcanonical or “molecular dynamics” techniques [10]. As the primary focus of this article is the elucidation of the Langevin approach, only a brief comparison with the simplest Monte Carlo method is made.

The details of the Monte Carlo calculation are as follows. First, the real and imaginary parts of the action are separated:

$$S = S_R + iS_I \quad (4.1)$$

with [recall eq. (1.2) above]:

$$S_R \equiv \frac{1}{2} \epsilon \delta \sum_{i=1}^N x_i^2 + \frac{1}{2} (x_1^2 + x_N^2), \quad (4.2a)$$

$$S_I \equiv \frac{1}{2\delta} \sum_{\langle i,j \rangle} (x_i - x_j)^2 - \frac{1}{2}\delta \sum_{i=1}^N x_i^2, \quad (4.2b)$$

where N , δ , and ϵ are parameters, and the notation $\langle i, j \rangle$ refers to all nearest-neighbor pairs i, j summed *once*.

Expectation values of functionals ϑ (corresponding to operators $\hat{\vartheta}$) in the ensemble governed by eq. (4.1) are given by

$$\langle \vartheta \rangle = \frac{\langle \vartheta e^{iS_I} \rangle_R}{\langle e^{iS_I} \rangle_R}, \quad (4.3)$$

where

$$\langle \vartheta' \rangle_R = \frac{\int D\mathbf{x} \exp(-S_R) \vartheta'}{\int D\mathbf{x} \exp(-S_R)}. \quad (4.4)$$

The expectation values of eq. (4.4) are generated easily, since random numbers obeying a gaussian distribution can be generated rapidly from the closed-form expression eq. (3.3).

A sample calculation with N equal to 50 and δ equal to 0.25 was performed. For ϵ equal to 100, less than one hundred updates of the entire system were required to give a value of

$$\frac{1}{N} \left\langle \sum_{i=1}^N x_i^2 \right\rangle \quad (4.5)$$

correct to one digit. This same level of accuracy required on the order of one million updates for ϵ equal to 50. These results suggest that the desired limit of small ϵ is at best obtainable with extreme difficulty by this most naïve Monte Carlo method. This is as it should be, for Monte Carlo methods are predicted upon the idea of importance sampling, and the limit of small ϵ is the limit in which this importance sampling is least effective.

5. Conclusions

In this paper we have studied analytically how the lattice free-field propagator behaves as a function of T (the volume of space time), δ (the lattice spacing) and ϵ (the Feynman cutoff). We found that at fixed finite volume an excellent approximate to the continuum can be had for moderate ϵ . A Langevin simulation relaxed to the known results with relaxation time $\tau \propto 1/\epsilon$ as predicted by analytic results.

For the anharmonic oscillator case we found that the simulations had the same behavior as in free-field theory in that the relaxation time was still of order $1/\epsilon$ and for finite volume the optimum ϵ was similar to the free-field case. This demonstrates

that Langevin simulations for interactive field theories in Minkowski space are possible with two extra costs over euclidean simulations. First, for the propagator the relaxation time is $1/\epsilon$ independent of momenta instead of $1/(p^2 + m^2)$. Second, one must do simulations at several ϵ and use that ϵ which maximizes $\langle \phi^2 \rangle$ to calculate the various Green functions.

References

- [1] M. Creutz, L. Jacobs, and C. Rebbi, *Phys. Reports* 95, (1983) 201;
J. Kogut, *Rev. Mod. Phys.* 55 (1983) 775;
D.J.E. Callaway, Los Alamos preprint LA-UR-84-3484, to appear in *Contemporary Physics*
- [2] E.L. Abers and B.W. Lee, *Phys. Reports* 9C (1973), 1;
J.C. Taylor, *Gauge theories of the weak interactions* (Cambridge, New York, 1976)
- [3] G.I. Parisi and Y.S. Wu, *Scientia Sinica* 24 (1981) 483;
B.I. Halperin and P.C. Hohenberg, *Rev. Mod. Phys.* 49 (1977) 435
- [4] J.R. Klauder, *Acta Phys. Austriaca, Suppl.* XXV (1983) 251;
C.M. Bender, F. Cooper, and B. Freedman, *Nucl. Phys.* B219 (1983) 61
- [5] P.M. Morse and H. Feshbach, *Methods of theoretical physics* (McGraw-Hill, New York, 1953)
- [6] J.R. Klauder and W.P. Peterson, Spectrum of certain nonself-adjoint operators and solutions of Langevin equations with complex drift, *J. Stat. Phys.*, in press
- [7] H. Hüffel and P.H. Rumpf, *Phys. Lett.* 148B (1984) 104
- [8] E. Helfand, *Bell System Tech. Jour.* 58 (1979) 2289
- [9] K. Binder, *Phase transitions and critical phenomena*, eds. C. Domb and M.S. Green, vol. 5B (Academic Press, NY, 1976);
N. Metropolis, A.W. Rosenbluth, M.N. Rosenbluth, A.H. Teller, and E. Teller, *J. Chem. Phys.* 21 (1953) 1087
- [10] D.J.E. Callaway and A. Rahman, *Phys. Rev. Lett.* 49 (1982) 613; *Phys. Rev. D28* (1983) 1506